COMPARISON OF DIFFERENT CRATER COUNTING METHODS APPLICATED TO PARANA VALLES. S.Bouley[1,2,3], R.A. Craddock[2], N.Mangold[3] and V. Ansan[3]. [1]Center for Earth and Planetary Studies, National Air and Space Museum, Smithsonian Institution, Washington D.C. 20560-0315, [2]IDES UMR8148, Bat. 509, Université Paris XI, 91405 Orsay Cedex, France (sylvain.bouley@u-psud.fr), [3]LPGNantes UMR6112 CNRS 44322 Université Nantes, France.

Introduction: Martian valley networks are good indicators of the past climate. These features are located primarily in heavily cratered terrain of Noachian age (>3.7 Ga) [1] but the exact timing of these features is not well understood. Recent global studies using superposed craters along different fluvial valleys [2, 3] determined that most formed during the Late Noachian to Early Hesperian. However, valley networks are small, linear features that make them difficult to accurately date using traditional crater-counting techniques. In this study, we set out to test the reliability of the counting methods used in [2] and [3] while comparing the results to other methods using fine scale age determination from small diameter craters. We applied these different methods to Parana Valles using a large dataset of high-resolution images from different instruments that allow us to count smaller craters while providing a good sampling of crater populations that is necessary to reduce uncertainties in age determination.

Dataset: We used three different types of images to cover the Parana Valles study area, including CTX (6m/pixel) and THEMIS visible images (17 to 35m/pixel), which provided optimal resolution for part of the study area. Where there were no available high resolution images, we used THEMIS IR night time images (100 m/pixel). The mosaic of all these images was used to map the Parana Valles network and to count craters. Additionally, we used digital topography from MOLA at a resolution of 460 m/pixel to delineate drainage basin and subbasin divides using automatic techniques established for digital elevation data of terrestrial watersheds [4].

Parana Valles Basin: We studied a large subbasin of the Parana Valles drainage system that is located upstream from the Parana/Loire basin and situated between Margarifer and Noachis Terra. The study covers an area equal to 26 452 km² and is drained by 3586 km of valleys organized dendritically (Fig. 1). This results in a drainage density of 0.13 km^{-1}, and we determined that the highest order stream is a 6^{th} order using the Strahler system [5]. The primary network is divided into two main branches where the source areas are located between 400 and 700 m elevation and terminate at an elevation of -1000 m. Two different morphologies are observed in the main tributaries. Between -1000 and 200 m elevation the valley is rectangular with a width of ~2 km. We observed that this valley is partially filled by eolian deposits. At an elevation of ~200 m, the main valley in the southern branch, becomes wider (between 3 and 8 km), exhibits a wide V-shape profile and incises interfluves. We suggest that the differences in morphology are the result of variation of lithology.

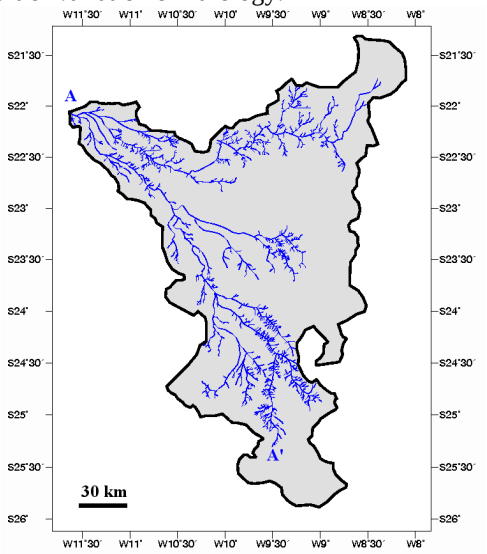

Figure 1. Parana subbasin and its drainage. AA' corresponds to the location of the longitudinal profile shown in Figure 3

Crater counting and dating methods: The first method we tested is the "buffered" method described by [2] and [3], which consists of counting craters down to 1 km that overlap at least partially with the valley. The second method we refer to as the "basin method," where we counted all the craters down to 350 meters located inside individual subbasins. The third method we refer to as the "interior valley method" where all craters >125 m in diameter and located within the valley walls are counted. These different methods permitted us to consider a large range of crater diameters and counting areas. To determine the absolute age, we calculated incremental crater densities using the Hartmann diagram [6] (Fig.2). We also calculated N(1) values to determine the formation period of the valley using established crater density boundaries [7].

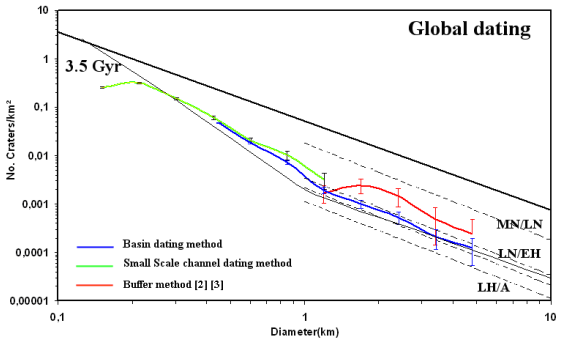

Figure 2. Incremental crater densities reported on Hartmann diagram [5]. The solid black line is the 3.5 Gyr boundary and dash lines represent the epoch boundaries. (MN: Middle Noachian, LN: Late Noachian, EH: Early Hesperian, LH: Late Hesperian, A: Amazonian).

Crater counts results: Figure 2 shows the incremental crater densities as determined by the three different methods. The results found with the buffered method are represented by the red curve and yield a Late Noachian age. However, this result is not consistent with the age determined by the two other methods. The basin method (blue line) yields an Early Hesperian age, and the corresponding incremental ages parallel the 3.5 Gyr line. The interior valley method (green line) yields a Late Noachian to Early Hesperian age. The diminution of crater densities at the smallest crater diameters can be explained by burial by an eolian deposit. Note that on this diagram the error bars are larger for the buffer method than the others, illustrating that while this technique can be applied quickly and is particularly useful for areas lacking higher resolution images the accuracy is not as high.

Method	Int. Channel	Basins	Buffer
Sup (km²)	2194	23765	4096
N(0,12)	1612	–	–
N(0,12) craters/km²	**0,735**	–	–
±	0,018	–	–
N(0,35)	206	1825	–
N(0,35) craters/km²	**0,094**	**0,077**	–
±	0,0065	0,0018	–
N(1)	7	91	26
N(1) craters/km²	**0,0043**	**0,0038**	**0,0063**
±	0,0012	0,0004	0,0012
Age period	**LN to EH**	**EH**	**LN**

Table 1. N(0.12), N(0.35) and N(1) values with uncertainties and determined age period using three different methods.

The cumulative N(1) values presented in Table 1 are consistent with ages determined from the Hartman diagram. We note that the basin method reduces the amount of uncertainty because of the larger crater sampling. Specifically, the basin method used 91 craters down to 1 km, and the buffered method used only 26 craters. This lower sampling of craters can explained the overestimation of the age of formation.

Variation of crater density: We studied the variation of crater densities N(0.125) on the bottom of the valley along the path AA' (Fig.1 and 3). The MOLA profile shows a change in slope (0.6 to 0.3%) at ~200 m elevation, which may also reflect variations in lithology. At elevations of <200 m, N(0.125) values are between 0 and 0.4 craters/km². These low values can be explained by an eolian deposit that was observed covering small craters. N(0.125) values increase at elevations >200 m. This crater density difference can be explained by the possibility that the morphology of valleys and local lithology do not support the generation or containment of an eolian deposition. The smaller diameter craters also suggest that this deposit becomes thicker downstream from the source.

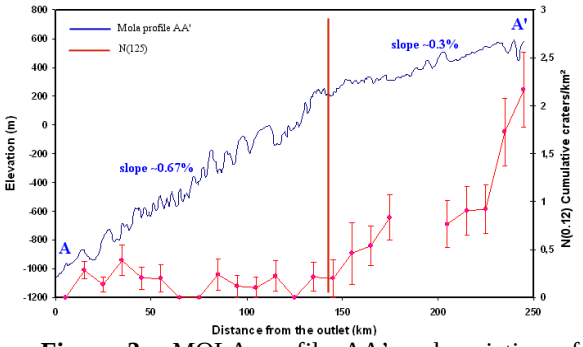

Figure 3. MOLA profile AA' and variation of N(0.125) calculated for the bottom of the valley

Conclusions: Our study demonstrates that the buffered crater counting method is more reliable in areas where the counting area is large, and it is possible that valley network ages presented in [2] and [3] may be off slightly. We also showed that crater densities measured inside valleys may be influenced by processes, such as eolian deposition, that occurred subsequent to valley network formation. In general the basin method provides a more reliable age estimate providing there is sufficient image resolution, but it requires an extra step in determining the location of the drainage divides.

References: [1] Milton D. J (1973) *JGR*, 78, 4037–4047. [2] Fasset C.I. and Head J.W. (2008) *Icarus*, 195, 61-89. [3] Hoke M.R.T. (2007) *LPS XXXVIII*, Abstract #1209. [4] Martz L.W. and Garbrecht J. (1992) *Computers and Geoscience*, **8**, 747-761. [5] Strahler A.N. (1952a) *Geol. Soc. Am. Bull*, 63, 898-912. [6] Hartmann W.K. (2005) *Icarus*, 174, 294-320. [7] Tanaka K.L. (1986) *JGR*, 91, 139-158.